Inorg. Chem. **2002**, *41*, 4952–4960

Matrix Reactivity of AlF and AlCl in the Presence of HCl and HBr: Generation and Characterization of the New Al(III) Hydrides HAlFCl, HAlFBr, and HAlClBr and the Monomeric Mixed Al(III) Halides AlX_2Y (X, Y = F, Cl, or Br)†

Hans-Jörg Himmel,* Jan Bahlo, Michael Haussmann, Fabian Kurth, Gregor Stösser, and Hansgeorg Schnöckel

Lehrstuhl für Analytische Chemie, Institut für Anorganische Chemie, Universität Karlsruhe, Engesserstrasse, Geb. 30-45, 76128 Karlsruhe, Germany

Received April 15, 2002

The spontaneous and photolytically induced reactions of AlF and AlCl in the presence of HCl and HBr in solid argon matrices were followed and the products identified and characterized by means of IR spectroscopy. Quantum mechanical calculations allow for a further evaluation of the properties of the reaction products. These are the adducts AlF·HCl, AlF·HBr, and AlCl·HBr, representing the products of spontaneous reactions, and the trivalent Al(III) hydrides HAlFCl, HAlFBr, and HAlClBr, which were formed upon photoactivation of these complexes. All three hydrides are planar molecules (C_s symmetry) with bond angles in agreement with the predictions of the VSEPR theory. In addition, the mixed halides $AlFCl_2$, $AlFBr_2$, and $AlClBr_2$ were formed upon photolysis. The bisadducts $AlF·(HCl)_2$ and $AlF·(HBr)_2$ are likely to be the precursors to these species.

Introduction

The recent years witnessed the characterization of several new hydrides of group 13 elements. These compounds are of considerable interest because of their potential to act as metal sources in chemical vapor deposition (CVD) processes,[1] and because of their structural richness.[2] Hydrides show a remarkable mutability, and the H atom can carry either a formally negative or positive partial charge and the element−H bonds can be either terminal or bridging. Stable adducts of MH_3 are now known not only for M = B, Al, or Ga but also, more recently, for In, e.g. $(cyclohexyl)_3P·InH_3$.[3] Without the stabilization by a suitable base, molecular hydrides of the group 13 elements with the formula MH_3 are known only in the form of dimers $(MH_3)_2$ for M = B or Ga to be accessible via synthetic routes.[4] There are also known species such as H_2GaBH_4 featuring two different group 13 atoms.[5] Although Ga_2H_6 is stable in the gas phase and has a sufficiently high vapor pressure for applications in CVD processes, it is difficult to handle and decomposes at temperatures higher than −20 °C. The monomers MH_3 can be generated and characterized only in inert gas matrices, e.g. by reaction of the metal atoms with molecular and/or atomic hydrogen (see eq 1).[6,7] Matrix isolation has also

$$M + H_2 \xrightarrow{h\nu} MH_2 \xrightarrow{h\nu} MH \xrightarrow[H_2]{h\nu} MH_3 \qquad (1)$$

proved to be extremely useful to study new monomer compounds bearing the formula H_2MX and HMX_2, where X represents a halogen atom. Thus H_2GaCl[8] and H_2InCl[9]

* Author to whom correspondense should be addressed. E-mail: himmel@achpc9.chemie.uni-karlsruhe.de.

† Dedicated to Professor Rüdiger Mews on the occasion of his 60th birthday.

(1) See, for example: Downs, A. J., Ed. *Chemistry of Aluminium, Gallium, Indium and Thallium*; Blackie: Glasgow, U.K., 1993.
(2) Aldridge, S.; Downs, A. J. *Chem. Rev.* **2001**, *101*, 3305.
(3) Hibbs, D. E.; Jones, C.; Smithies, N. A. *J. Chem. Soc., Chem. Commun.* **1999**, 185.
(4) Downs, A. J.; Goode, M. J.; Pulham, C. R. *J. Am. Chem. Soc.* **1989**, *111*, 1936−1937. Pulham, C. R.; Downs, A. J.; Goode, M. J.; Rankin, D. W. H.; Robertson, H. E. *J. Am. Chem. Soc.* **1991**, *113*, 5149−5162.
(5) Pulham, C. R.; Brain, P. T.; Downs, A. J.; Rankin, D. W. H.; Robertson, H. E. *J. Chem. Soc., Chem. Commun.* **1990**, 177. Downs, A. J.; Greene, T. M.; Johnson, E.; Brain, P. T.; Morrison, C. A.; Parsons, S.; Pulham, C. R.; Rankin, D. W. H.; Aarset, K.; Mills, I. M.; Page, E. M.; Rice, D. A. *Inorg. Chem.* **2001**, *40*, 3484.
(6) Kurth, F. A.; Eberlein, R. A.; Schnöckel, H.; Downs, A. J.; Pulham, C. R. *J. Chem. Soc., Chem. Commun.* **1993**, 1302.
(7) Pullumbi, P.; Bouteiller, Y.; Manceron, L.; Mijoule, C. *Chem. Phys.* **1994**, *185*, 25.
(8) Köppe, R.; Schnöckel, H. *J. Chem. Soc., Dalton Trans.* **1992**, 3393.

10.1021/ic020275a CCC: $22.00
Published on Web 08/23/2002

are among the species with the formula H_2MX which were generated and characterized in matrix isolation experiments by reaction of MX with dihydrogen. $HAlCl_2$,[10] $HGaCl_2$,[11] and $HInCl_2$,[9] the products of the photoinduced reactions of the subvalent MX species with HX (see eq 2), are known representatives of compounds with the formula HMX_2.[12]

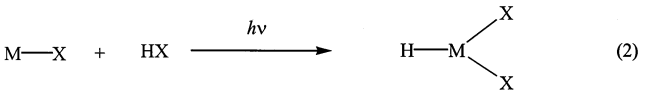

(2)

Herein we will report on the spontaneous and photolytically induced matrix reactions of AlCl with HBr and of AlF with HCl and HBr. The spontaneous reactions lead to the adducts AlCl·HBr, AlF·HCl, and AlF·HBr. Further reactions can be set in train by the action of photolysis. It has been shown previously that the effect of photolysis is to excite the subhalide from its singlet electronic ground state into its triplet excited state.[13] These reactions lead to representatives of the general formula HAlXY, where X and Y are two different halogen atoms, namely, HAlClBr, HAlFCl, and HAlFBr. Additionally, $AlClBr_2$, $AlFCl_2$, and $AlFBr_2$ are formed. The results of this study shed light not only on the properties of all these compounds, but also on the reaction pathways leading to them and to the Al(III) trihalides. The knowledge of these pathways is most likely of relevance for a better understanding of the mechanism of Al oxidation by HX (X = F, Cl, or Br) leading in several steps finally to AlX_3.

Experimental Section

In the matrix experiments argon gas containing up to 5% of HCl or HBr was sprayed slowly and typically over a period of 1 h at relatively low pressures (5×10^{-5} mbar) onto a polished copper block kept at 12 K by means of a closed cycle refrigerator (Leybold LB 510). The flow of the gas was controlled by a needle valve. AlF and AlCl were generated by passing CHF_3 or HCl, respectively, over aluminum (Merck, 99.999%) in a Knudsen-type graphite cell, heated resistively to 900 °C. Hence the AlF or AlCl vapor emitted from the cell was co-deposited together with HCl or HBr in an excess of Ar onto the copper block. Other details of the relevant procedures have been described elsewhere.[14]

HCl (Messer, 99.995%), HBr (Messer, 99.98%), and CHF_3 (Messer, 99.995%) were used as supplied and with the quoted purities. DCl and DBr were prepared by reaction of D_2O with $SiMe_3Cl$ and PBr_3, respectively, followed by trap-to-trap distillation. The purity was checked by gas-phase IR measurements.

Infrared spectra of the matrix samples were recorded on a Bruker 113v FTIR instrument equipped with a liquid N_2-cooled MCT detector, covering the spectral range 4000−400 cm^{-1}, and a DTGS detector for measurements in the spectral range 700−200 cm^{-1}. A resolution of 0.5 and 1.0 cm^{-1} was used for measurements with the MCT and DTGS detector, respectively.

UV photolysis (λ_{max} = 254 nm) of the matrices was achieved by the aid of a low-pressure Hg lamp (Graentzel, Karlsruhe) operating at 200 W, the radiation being transmitted through a quartz window.

Density Functional Theory (DFT) and ab initio quantum chemical calculations were performed with the TURBOMOLE program package,[15] applying the BP86 and the MP2 methods in combination with an SVP type basis set. Normal coordinate analysis relied on the program ASYM 40.[16]

Results

AlCl and HBr. Experiments in which AlCl was co-deposited together with HBr in an excess of argon gave evidence for a sharp and strong IR band at 454 cm^{-1} immediately upon deposition due to AlCl monomers. In addition to this band, the spectrum contained a somewhat broader absorption at 425 cm^{-1} and a weaker one at 2420 cm^{-1} belonging to a first product **1a** of the reaction of AlCl with HBr (see Figures 1 and 2). There followed a period of UV photolysis of the matrix. In the IR spectrum taken after this photolysis treatment (see Figure 2), the absorption due to product **1a** was observed to decrease. At the same time, several new absorptions appeared. One group of bands, located at 1959.6, 644.2, 552.4/547.7, 462.1, and 404 cm^{-1}, can be assigned to a second distinct reaction product **2a**. There also were two new bands at 588 and 511 cm^{-1} belonging to a third product **3a**. Finally, two weak features appeared at 616.1 and 560.1 cm^{-1} due to a fourth product **4a**.

The experiment was repeated, but now with DBr in place of HBr. The IR spectrum taken upon co-deposition of AlCl and DBr in an excess of solid argon gave evidence of one absorption attributable to the D-version of product **1a**. At 425 cm^{-1}, the wavenumber was not significantly affected by H/D substitution. By analogy with the experiments conducted with HBr, UV photolysis brought about the decrease of the absorption due to **1a**. At the same time, new absorptions were seen to grow in. Four of these, at 1425, 560/566, 410, and 400 cm^{-1}, are attributable to the D-version of product **2a**. The wavenumbers of all observed vibrational modes and their response to photolysis are included in Table 1.

Finally, experiments were conducted with different concentrations of HBr in the matrix. The same absorptions were detected in these experiments, but the relative intensities of the absorptions belonging to different products **1a**−**4a** varied. For low concentrations of HBr in the matrix (2%), the intensities of all absorptions were reduced. However, the

(9) Himmel, H.-J.; Downs, A. J.; Greene, T. M. *J. Am. Chem. Soc.* **2000**, *122*, 922.
(10) Schnöckel, H. *J. Mol. Struct.* **1978**, *50*, 275.
(11) Köppe, R.; Tacke, M.; Schnöckel, H. *Z. Anorg. Allg. Chem.* **1991**, *605*, 35.
(12) $HAlBr_2$ was also sighted in matrix isolation experiments, but generated via a different route. See: Müller, J.; Wittig, B. *Eur. J. Inorg. Chem.* **1998**, 1807.
(13) Himmel, H.-J. *J. Chem. Soc., Dalton Trans.* **2002**, 2678.
(14) Schnöckel, H.; Schunck, S. *Chem. Unserer Zeit* **1987**, *21*, 73.
(15) Ahlrichs, R.; Bär, M.; Häser, M.; Horn, H.; Kölmel, C. *Chem. Phys. Lett.* **1989**, *162*, 165. Eichkorn, K.; Treutler, O.; Öhm, H.; Häser, M.; Ahlrichs, R. *Chem. Phys. Lett.* **1995**, *240*, 283. Eichkorn, K.; Treutler, O.; Öhm, H.; Häser, M.; Ahlrichs, R. *Chem. Phys. Lett.* **1995**, *242*, 652. Eichkorn, K.; Weigend, F.; Treutler, O.; Ahlrichs, R. *Theor. Chem. Acc.* **1997**, *97*, 119. Weigend, F.; Häser, M. *Theor. Chem. Acc.* **1997**, *97*, 331. Weigend, F.; M. Häser, M.; Patzelt, H.; Ahlrichs, R. *Chem. Phys. Lett.* **1998**, *294*, 143.
(16) ASYM 40, version 3.0, upgrade of program ASYM 20; Hedberg, L.; Mills, I. M. *J. Mol. Spectrosc.* **1993**, *160*, 117.

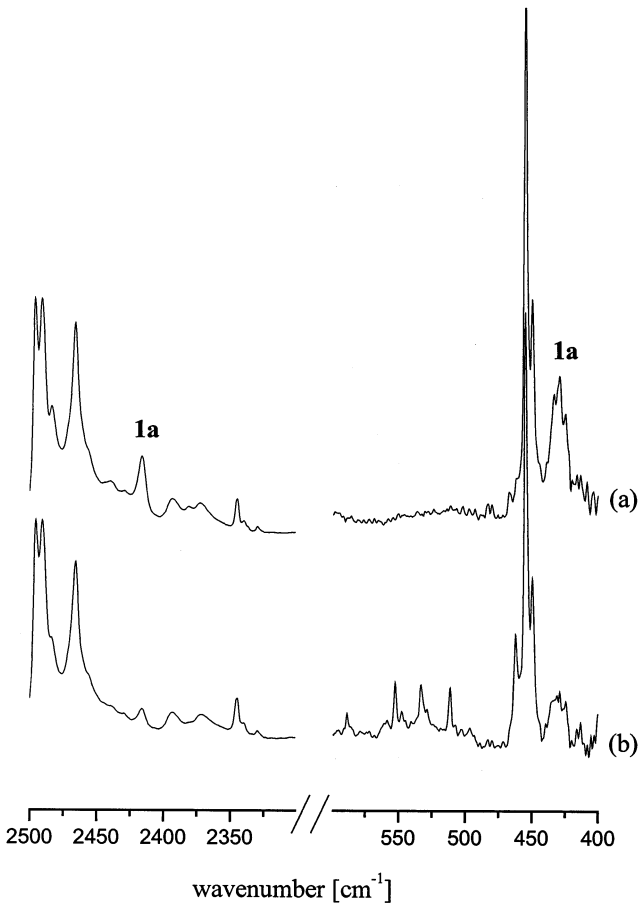

Figure 1. IR spectrum taken for an Ar matrix containing AlCl and HBr (a) before photolysis and (b) following UV photolysis (λ_{max} = 254 nm).

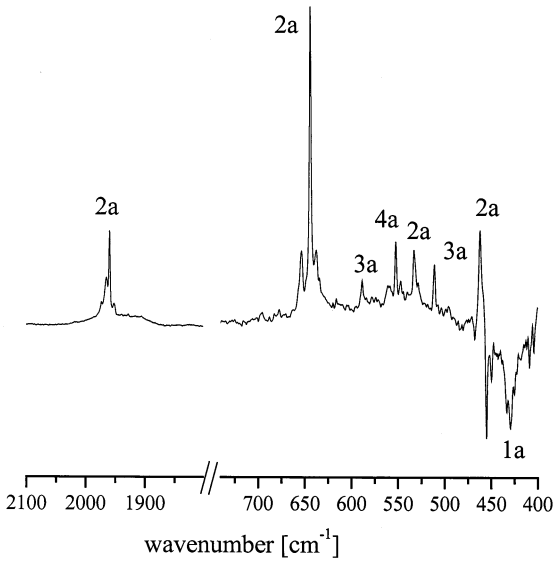

Figure 2. IR difference spectra taken for an Ar matrix containing AlCl and HBr after UV photolysis (λ_{max} = 254 nm) minus before photolysis.

bands due to species **2a** and **4a** gained intensity relative to the ones due to species **3a**. This might imply that **2a** and **4a** are the products of reactions with *one* HBr moiety, while **3a** is formed by reaction with *two* moieties of HBr or, more likely, with the dimer $[HBr]_2$.

Table 1. Observed Wavenumbers (cm^{-1}) for a Matrix Containing AlCl and HBr/DBr in an Excess of Ar before and after UV Photolysis (λ_{max} = 254 nm)

HBr	DBr	deposition[a]	photolysis[a]	absorber
2420	*b*	↑	↓	**1a**
1959.6	1425		↑	**2a**
644.2	566/560			
616.1	616.1		↑	**4a**
588.3	588.3		↑	**3a**
560.1	560.1		↑	**4a**
552.4/547.7	566/560		↑	**2a**
511.0	511.0		↑	**3a**
462.1	*b*		↑	**2a**
454	454	↑	↓	AlCl
425	425	↑	↓	**1a**
404	410		↑	**2a**
272	272	↑	↓	$(AlCl)_2$

[a] ↑ = increase in intensity. ↓ = decrease in intensity. [b] Too weak to be detected, obscured by more intense absorptions, or outside the range of detection.

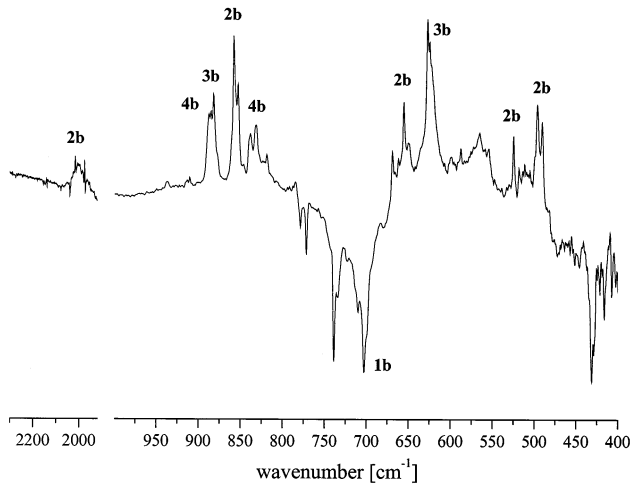

Figure 3. IR difference spectra taken for an Ar matrix containing AlF and HCl after UV photolysis (λ_{max} = 254 nm) minus before photolysis.

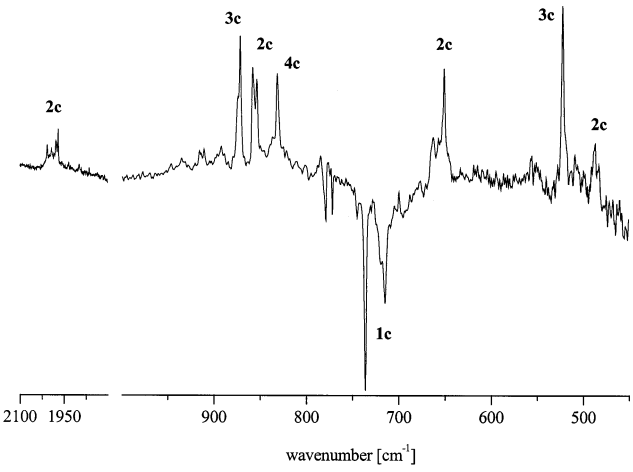

Figure 4. IR difference spectra taken for an Ar matrix containing AlF and HBr after UV photolysis (λ_{max} = 254 nm) minus before photolysis.

AlF and HCl. The spectra taken upon co-deposition of AlF together with 3% HCl in an excess of argon are displayed in Figure 3. They are dominated by sharp absorptions due to HCl, AlF, and $(AlF)_2$[17] near 2854, 776.3/772.4, and 431.0 cm^{-1}. In addition, the spectrum contained new

Table 2. Observed Wavenumbers (cm^{-1}) for a Matrix Containing AlF and HCl/DCl in an Excess of Ar before and after UV Photolysis (λ_{max} = 254 nm)

HCl	DCl	deposition[a]	photolysis[a]	absorber
2721.4	1903.9	↑	↓	**1b**
2005	1437.9		↑	**2b**
887.1/884.7	887.1/884.7		↑	**4b**
881.7	882.1		↑	**3b**
857.8/852.5	856.4/850.9		↑	**2b**
831.3	832.5		↑	**4b**
776.3/772.0	776.3/772.0	↑	↓	AlF
743.1/736.2	733.3	↑	↓	**1b**
714.8	709.7	↑	↓	**1b**
655.1	538.3		↑	**2b**
627.1/624.3	627.1/624.3		↑	**3b**
524.6	*b*		↑	**2b**
496.2/490.1	*b*		↑	**2b**
430.1	430.1	↑	↓	$(AlF)_2$

[a] ↑ = increase in intensity. ↓ = decrease in intensity. [b] Too weak to be detected, obscured by more intense absorptions, or outside the range of detection.

Table 3. Observed Wavenumbers (cm^{-1}) for a Matrix Containing AlF and HBr/DBr in an Excess of Ar before and after UV Photolysis (λ_{max} = 254 nm)

HBr	DBr	deposition[a]	photolysis[a]	absorber
2419.3	1742.9	↑	↓	**1c**
1990	1455		↑	**2c**
873.6	874.0		↑	**4c**
871.1	871.1		↑	**3c**
858.5/853.8	851.9/846.3		↑	**2c**
831.1	831.1		↑	**4c**
776.3/772.0	776.3/772.0	↑	↓	AlF
736.2	735.9	↑	↓	**1c**
650.5	488.1		↑	**2c**
522.2	522.2		↑	**3c**
486.8	*b*		↑	**2c**
430.1	430.1	↑	↓	$(AlF)_2$

[a] ↑ = increase in intensity. ↓ = decrease in intensity. [b] Too weak to be detected, obscured by more intense absorptions, or outside the range of detection.

absorptions at 743.1/736.2 and 714.8 cm^{-1}, which can be assigned to a first, spontaneously formed product **1b** of the reaction of AlF with HCl. Following 10 min of UV photolysis (λ_{max} = 254 nm) of the matrix, the IR spectra witnessed the decrease of the bands associated with product **1b** and the simultaneous appearance of several new absorptions. One group of absorptions consisted of not less than five bands, located at 2005, 857.8/852.5, 655.1, 524.6, and 496.2/490.1 cm^{-1}, all belonging to the same absorber **2b**, representing a second product of the reaction of AlF with HCl. Two new absorptions at 881.7 and 627.1/624.3 cm^{-1} can be assigned to a third product **3b**. Finally, two broad and weak bands appeared at 887.1/884.7 and 831.3 cm^{-1} and were assigned to a fourth species **4b**.

An additional experiment was carried out with DCl in place of HCl. The spectrum taken upon deposition gave again evidence for absorptions due to a first, spontaneously formed product **1b** of the reaction of AlCl with DCl, now in its deuterated version. These were located at 733.3 and 709.7 cm^{-1}. In the same way as already reported for the reaction of AlCl with HBr, additional products can be generated upon exposure of the matrix to UV photolysis. All bands assigned to product **2b** were observed to shift toward lower wavenumbers. The largest effect was observed for the band at 2005 cm^{-1}, which shifted to 1437.9 cm^{-1}, giving a ν(H)/ν(D) ratio of 1.3944:1. The band at 857.8/852.5 cm^{-1} in the experiments with HCl experienced only a small shift to 856.4/850.9 cm^{-1}. The band at 655.1 cm^{-1} was now observed at 538.3 cm^{-1} [ν(H)/ν(D) = 1.2170:1]. Unfortunately, the spectra failed to give any sign of the D-counterparts of the bands at 524.6 and 496.2/490.1 cm^{-1}, which were observed in the experiments with HCl and belong to species **2a**. The failure to detect these absorptions is caused either by lack of intensity or by the absorptions being outside the range of detection of our experiments. The two bands due to species **3a** showed no shifts, and this possibly implies that they do not contain hydrogen. The two weak features at 887.1/884.7 and 831.3 cm^{-1} were also not affected by substitution of HCl by DCl.

AlF and HBr. The reaction of AlF with HBr was observed to follow the same pattern as the reaction with HCl. Thus, a new absorption *red*-shifted from that of AlF at 736.2 cm^{-1} was present in the IR spectrum taken immediately upon codeposition and can be assigned to a first product **1c**, the Br analogue of **1b**. Following 10 min of UV photolysis (λ_{max} = 254 nm), this band decreased and gave way to several new absorptions. These were located near 1990 cm^{-1} and at 858.1/853.8, 650.5, and 486.8 cm^{-1}, all belonging to a common absorber **2c**. Additional absorptions due to a third species **3c** were observed at 871.1 and 522.2 cm^{-1}. Finally, the spectrum witnessed the appearance of two weaker features at 873.6 and 831.1 cm^{-1} due to a fourth species **4c**.

In the experiments with DBr in place of HBr, the IR spectra again showed an absorption immediately following deposition due to **1c** in its D-version. At 735.9 cm^{-1}, the wavenumber was only slightly shifted with respect to that detected in the experiment with HBr. Upon UV photolysis, the bands due to **1c** again decreased and several new bands were seen to grow in, belonging to the D-equivalents of products **2c**, **3c**, and **4c**. The bands due to product **2c** were all *red*-shifted. Thus the band at 1990 cm^{-1} in the experiment with HBr appeared at 1455 cm^{-1} in the experiments with DBr, giving a ν(H)/ν(D) ratio of 1.3677:1. The band at 650.5 cm^{-1} was now observed at 488.1 cm^{-1} [ν(H)/ν(D) = 1.3327:1]. The smallest shift was monitored for the absorption at 858.5/853.8 cm^{-1}, which now occurred at 851.9/ 846.3 cm^{-1}. The D-counterpart of the absorption at 486.8 cm^{-1} escaped detection, most likely because of lack of intensity. Species **3c** again gave rise to two absorptions, with wavenumbers similar to those observed in the experiment with HBr (871.1 and 522.2 cm^{-1}). As with **3c**, the absorptions due to **4c** exhibited no significant changes and were observed at 873.6 and 831.1 cm^{-1}. The obvious inference is that **3c** and **4c**, like **3a**,**b** and **4a**,**b**, do not contain hydrogen.

Discussion

On the basis of the IR spectra, comparison with related species, and the results of quantum mechanical calculations applying ab initio (MP2) as well as DFT (BP86) methods,

(17) Ahlrichs, R.; Zhengyan, L.; Schnöckel, H. *Z. Anorg. Allg. Chem.* **1984**, *519*, 155.

HAlClBr (**2a**), HAlFCl (**2b**), and HAlFBr (**3c**) will be shown to be the primary products of the photolytically induced reactions of AlCl with HBr and of AlF with HCl or HBr, respectively. The experiments give also evidence for the presence of the complexes AlF·HCl (**1a**), AlF·HBr (**1b**), and AlCl·HBr (**1c**), formed immediately upon deposition, and which most likely act as precursors to HAlFCl, HAlFBr, and HAlClBr, respectively. The photoinduced reactions result in the additional formation of $AlFCl_2$, $AlFBr_2$, and $AlClBr_2$ (**3a**−**c**). One possible route to these species starts from the bisadducts AlF·$(HCl)_2$, AlF·$(HBr)_2$, and AlCl·$(HBr)_2$, which, however, escaped detection in our experiments. Finally, **4a**−**c** will be shown to be the trivalent Al-halides AlX_2Y, which were formed in small quantities by reaction with traces of HF and HCl.[18] The adducts AlF·HF·HCl, AlF·HF·HBr, and AlCl·HCl·HBr are possible precursors to these species. All compounds will be discussed in turn, first the adducts AlX·HY (X = F or Cl or Y = Cl or Br), then the insertion products HAlXY, and finally the trihalides $AlXY_2$ and $AlYX_2$.

AlCl·HBr, AlF·HCl, and AlF·HBr, 1a−c. The absorptions due to **1a**−**c** are close to the absorptions of AlCl (in the case of **1a**) and AlF (in the case of **1b** and **1c**), but *red*-shifted by 29.6, 33.2/28.9, and 40.1/35.8 cm^{-1}. We anticipate the species responsible for these absorptions to be the adducts AlCl·HBr, AlF·HCl, and AlF·HBr, respectively, formed spontaneously upon deposition. Support for such an assignment comes from comparison with related species, namely the complexes AlCl·HCl,[10] GaCl·HCl,[11] and InCl·HCl,[9] which all were found to be formed immediately upon codeposition of the M(I) halides (M = Al, Ga, or In, respectively) with HCl in solid argon matrices. A possible structure for such an adduct was recently suggested by Tacke, Dunne, El-Gamati, Fox, Rous, and Cuffe on the basis of quantum chemical (DFT) calculations.[19]

HAlClBr, HAlFCl, and HAlFBr, 2a−c. Product **2a** of the photolytically induced reaction of AlCl with HBr is characterized by IR absorptions at 1959.6, 644.2, 552.4/547.7, 462.1, and 404 cm^{-1}. Of these, the absorption at 1959.6 cm^{-1} occurs in a region characteristic of the ν(Al−H) stretching vibration in Al(III) compounds (cf. $HAlCl_2$ 1967.6 cm^{-1},[10] H_2AlNH_2 1899.3/1891.0 cm^{-1},[20] H_2AlPH 1874.1/1866.1 cm^{-1} [21]). The absorptions at 552.4/547.7 and 404 cm^{-1} appear in regions where ν(Al−Cl) and ν(Al−Br) stretching modes are expected to show (cf. $HAlCl_2$ ν_{as} 578.9, ν_s 481.3[10] and $HAlBr_2$ ν_{as} 476.0, ν_s 366.0[22]). We thus anticipate **2a** to be the Al(III) hydride HAlClBr. Our calculations using DFT methods (BP86) resulted in a planar geometry with C_s symmetry for this molecule, which is characterized by Al−H, Al−Cl, and Al−Br distances of 1.5844, 2.1091, and 2.2610 Å, respectively, and H−Al−Cl, H−Al−Br, and Cl−Al−Br bond angles of 120.1°, 121.1°, and 118.9°. The trend of the bond angles (Br−Al−Cl < H−Al−Cl < H−Al−Br) is thus in full agreement with what is anticipated on the basis of simple VSEPR theory.[23] In Table 4 the wavenumbers calculated for the molecule in its optimum geometry and the two relevant isotopic forms are compared with the experimentally observed values. The comparison lends support to our assignment. The modes with high ν(Al−H), ν(Al−Cl), and ν(Al−Br) stretching mode character [ν_1(a′), ν_3(a′), and ν_4(a′)] were calculated to have wavenumbers of 1959, 552, and 438 cm^{-1}, respectively, in excellent agreement with the experimental values.

Table 4. Comparison between the IR Absorptions Observed and Calculated for HAlClBr and DAlClBr (**2a**), HAlFCl and DAlFCl (**2b**), and HAlFBr and DAlFBr (**2c**) [wavenumbers in cm^{-1}, with calculated IR intensities (in km mol^{-1}) in parentheses]

HAlClBr		DAlClBr		
exptl	calcd[a]	exptl	calcd[a]	assignment
1959.6	1959 (111)	1425	1423 (73)	ν_1(a′)
644.2	651 (243)	560/566	570 (196)	ν_2(a′)
552.4/547.7	552/547 (49)	*b*	451 (43)	ν_3(a′)
404	391 (34)	400	379 (23)	ν_4(a′)
b	134 (5)	*b*	133 (5)	ν_5(a′)
462.1	438 (91)	410	334 (59)	ν_6(a″)

HAlFCl		DAlFCl		
exptl	calcd[a]	exptl	calcd[a]	assignment
2005	1973.4 (93)	1437.9	1427.3 (63)	ν_1(a′)
857.8	859.9 (129)	856.4	856.8 (113)	ν_2(a′)
655.1	665.3 (123)	538.3	541.6 (116)	ν_3(a′)
524.6	524.9 (52)	*b*	465.3 (20)	ν_4(a′)
b	222.6 (19)	*b*	221.3 (19)	ν_5(a′)
496.2	478.8 (137)	*b*	376.4 (95)	ν_6(a″)

HAlFBr		DAlFBr		
exptl	calcd[a]	exptl	calcd[a]	assignment
1990	1964.6 (105)	1455	1420.5 (68)	ν_1(a′)
858.5	851.5 (121)	851.9	848.9 (109)	ν_2(a′)
650.5	654.3 (141)	488.1	493.6 (124)	ν_3(a′)
b	415.4 (51)	*b*	394.3 (20)	ν_4(a′)
b	203.0 (11)	*b*	200.6 (11)	ν_5(a′)
486.8	468.5 (120)	*b*	365.8 (82)	ν_6(a″)

[a] C_s symmetry. [b] Too weak to be detected, obscured by more intense absorptions, or outside the range of detection.

In its H-version, product **2b** gave rise to five absorptions located at 2005, 857.8, 655.1, 524.6, and 496.2/490.1 cm^{-1}. The broad absorption near 2005 cm^{-1} again occurs in a region characteristic of the stretching vibration of terminal Al(III)−H bonds. We thus anticipate **2a** to be the Al(III) hydride HAlFCl, formed by the photolytically induced reaction of AlF with HCl. Calculations with DFT methods (BP86) again predict a planar geometry with C_s symmetry for such a molecule. The Al−H, Al−F, and Al−Cl distances were calculated to be 1.5748, 1.6724, and 2.1022 Å, and the H−Al−F, H−Al−Cl, and F−Al−Cl angles 119.9°, 122.6°, and 117.5°, respectively. Again, the bond angles are in full agreement with the predictions of the VSEPR theory. The results of the frequency calculations are included in

(18) These traces are caused by incomplete reaction of liquid Al metal with an excess of HF or HCl, which passed the Knudsen cell (see Experimental Section).

(19) Tacke, M.; Dunne, J. P.; El-Gamati; Fox, S.; Rous, A.; Cuffe, L. P. *J. Mol. Struct.* **1999**, *447*, 221.
(20) Himmel, H.-J.; Downs, A. J.; Greene, T. M. *J. Am. Chem. Soc.* **2000**, *122*, 9793.
(21) Himmel, H.-J.; Downs, A. J.; Greene, T. M. *Inorg. Chem.* **2001**, *40*, 396.
(22) Müller, J.; Wittig, B. *Eur. J. Inorg. Chem.* **1998**, 1807.
(23) Gillespie, R. J.; Hargittai, I. *The VSEPR Model of Molecular Geometry*; Allyn and Bacon: Boston, MA, 1991. Gillespie, R. J. *Chem. Soc. Rev.* **1992**, *21*, 59.

Table 4, which compares the theoretical with the experimental values for the two isotopomers HAlFCl and DAlFCl. Our experiments hit on not less than five of the six vibrational fundamentals of HAlFCl and four of the fundamentals of DAlFCl. According to our calculations, the ν(Al−H) stretching vibration should occur at 1973.4 cm^{-1}, in satisfactory agreement with the observed wavenumber (2005 cm^{-1}). The ν(H)/ν(D) ratios calculated and observed (1.3826:1 and 1.3686:1, respectively) give support to this assignment. Next comes the mode with a high degree of ν(Al−F) character, located at 857.8 cm^{-1} in our experiments. Again the calculated wavenumber (859.9 cm^{-1}) is in excellent agreement with the experimental one and compares with a value of 892.4 cm^{-1} for the similar mode of $FAl(O_2)_2$.[24] The band at 655.1 cm^{-1} [ν(H)/ν(D) = 1.2170:1] in our experiments can then be assigned to a motion with a high contribution from the *in-plane* Al−H rocking fundamental, ν_3(a′). At 665.3 cm^{-1} [ν(H)/ν(D) = 1.2284:1] the calculated value is close to the experimental one. The observed wavenumber is also close to the wavenumber of the similar mode in $HAlCl_2$ (654.5 cm^{-1}). The ν_4(a′) mode, which can roughly be described as an *in-plane* deformation mode of HAlClF, is observed at 524.6 cm^{-1} and calculated to occur at 524.9 cm^{-1}. Additionally, the spectra gave evidence for an absorption at 496.2 cm^{-1} attributable to a mode with a high contribution from the *out-of-plane* Al−H bending mode, ν_6(a″), of HAlClF. The calculations predict a value of 478.8 cm^{-1} for this mode. The only vibration of HAlFCl that escaped detection was the ν_5(a′) mode, which is calculated to appear at 222.6 cm^{-1}, i.e., near the limit of detection in our experiments, and to carry very little intensity.

The circumstances of its formation and the wavenumbers of its vibrational modes suggest that **2c** is the Br equivalent

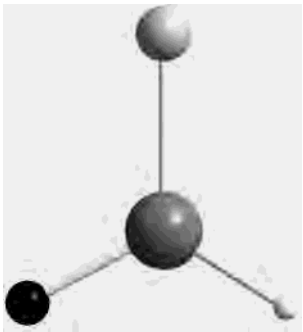

2b

of **2b**, namely the Al(III) species HAlFBr. DFT calculations resulted in a planar energy minimum structure with Al−H, Al−F, and Al−Br bond lengths of 1.5762, 1.6741, and 2.2551 Å and H−Al−F, H−Al−Br, and F−Al−Br angles of 119.3°, 122.7°, and 118.0°. Again the observed IR spectrum shows characteristic vibrational modes which lend support to our assignment. Table 4 compares the calculated and experimental wavenumbers for this species. The general level of agreement is pleasing. The mode at 1964.6 cm^{-1} [ν(H)/ν(D) = 1.3650:1] according to the calculations can again be assigned to the ν(Al−H) stretching fundamental, ν_1(a′), which was observed near 1990 cm^{-1} [ν(H)/ν(D) = 1.3650:1] in the experiments. Next comes the mode at 851.5 cm^{-1} [ν(H)/ν(D) = 1.0031:1] according to the calculations and 858.1 cm^{-1} [ν(H)/ν(D) = 1.0077:1] according to the experiments, exhibiting a high contribution from the ν(Al−F) stretching fundamental, ν_2(a′). The absorption at 654.3 cm^{-1} [ν(H)/ν(D) = 1.3256:1] in the calculations can again be assigned to a mode with *in-plane* Al−H rocking fundamental character, ν_3(a′), and the experimental wavenumber (650.5 cm^{-1}) and ν(H)/ν(D) ratio (1.3327:1) are in excellent agreement with the calculated values. The experiments succeeded also in detecting an absorption at 486.8 cm^{-1}, which is a strong candidate for the *out-of-plane* Al−H bending mode, ν_6(a″), calculated to appear at 468.5 cm^{-1}.

Normal Coordinate Analysis. On the basis of the experimentally observed wavenumbers, a normal coordinate analysis was carried out for each of the three hydrides HAlClBr, HAlFCl, and HAlFBr. The following six (not normalized) symmetry coordinates were used in this analysis: $S_1 = r$(Al−H), $S_2 = r$(Al−F), $S_3 = \delta$(H−Al−Y) − δ(H−Al−F), $S_4 = r$(Al−Y), $S_5 = \delta$(X−Al−F), $S_6 = \gamma$(H−Al−F−Y). For HAlClBr, a force constant f(Al−H) of 222 N m^{-1} was derived. This value is in good agreement with that derived previously for $HAlCl_2$ (219 N m^{-1}).[10] The force constant f(Al−Cl) of HAlClBr was determined to be 266 N m^{-1} and compares with values of 277, 274, and 292 N m^{-1} derived for $HAlCl_2$,[10] $AlCl_3$,[25] and ClAlO.[26] Finally, the normal coordinate analysis yielded a value of 223 N m^{-1} for the force constant f(Al−Br). Again, the agreement with the force constants in other Al(III) compounds featuring terminal Al−Br bonds is pleasing (cf. $AlBr_3$ 223 N m^{-1} [27] and $BrAlO_2$ 255 N m^{-1} [28]). For HAlFCl, force constants f(Al−H), f(Al−F), and f(Al−Cl) of 204, 476, and 327 N m^{-1} were derived. The value for f(Al−F) is in good agreement with those derived for f(Al−F) of FAlO (501 N m^{-1}),[26] AlF_3 (487 N m^{-1}),[29] and $FAl(O_2)_2$ (493 N m^{-1}).[24] The increase of the force constant f(Al−Cl) with respect to that of HAlClBr reflects the higher electronegativity of the fluorine ligand. Finally, HAlFBr is characterized by force constants f(Al−H), f(Al−F), and f(Al−Br) of 230, 423, and 248 N m^{-1}, respectively. The force constant f(Al−Br) is larger for HAlFBr than for HAlClBr, showing again the effect of the fluorine ligand.

$AlClBr_2$, $AlFCl_2$, and $AlFBr_2$, 3a−c. The spectra taken upon photolysis contained additional features at 588 and 511 cm^{-1} for AlCl and HBr, at 881.7 and 627.1 cm^{-1} for AlF and HCl, and at 871.1 and 522.2 cm^{-1} for AlF and HBr, which belong to a third reaction product **3a−c**. These absorptions exhibited no shift when HCl was replaced by DCl. Thus the product responsible for these absorptions is not likely to contain hydrogen. There is also no sign of any

(24) Bahlo, J.; Himmel, H.-J.; Schnöckel, H. *Angew. Chem.* **2001**, *113*, 4820; *Angew. Chem., Int. Ed.* **2001**, *40*, 4696.

(25) Schnöckel, H. *Z. Anorg. Allg. Chem.* **1976**, *424*, 203.
(26) Schnöckel, H. *J. Mol. Struct.* **1978**, *50*, 267.
(27) Beattie, I. R.; Horder, J. R. *J. Chem. Soc. A* **1969**, 2655.
(28) Bahlo, J.; Himmel, H.-J.; Schnöckel, H. *Inorg. Chem.* **2002**, *41*, 2678.
(29) McCory, L. D.; Paul, R. C.; Margrave, J. L. *J. Phys. Chem.* **1963**, *67*, 1986. Snelson, A. *J. Phys. Chem.* **1967**, *71*, 3201.

Table 5. Comparison between the IR Absorptions Observed and Calculated for $AlClBr_2$ (**3a**), $AlFCl_2$ (**3b**), and $AlFBr_2$ (**3c**) [wavenumbers in cm^{-1}, with calculated IR Intensities (in km mol^{-1}) in parentheses]

$AlClBr_2$ (**3a**)		$AlFCl_2$ (**3b**)		$AlFBr_2$ (**3c**)		
exptl	calcd[a]	exptl	calcd[a]	exptl	calcd[a]	assignment
511	498 (145)	881.7	880.5 (107)	871.1	865.0 (101)	$\nu_1(a_1)$
b	265 (2)	*b*	426.1 (7)	*b*	300.4 (6)	$\nu_2(a_1)$
b	98 (2)	*b*	147.8 (6)	*b*	102.5 (2)	$\nu_3(a_1)$
588	583 (132)	627.1	629.8 (181)	522.2	517.2 (184)	$\nu_4(b_1)$
b	116 (4)	*b*	201.9 (20)	*b*	210.1 (37)	$\nu_5(b_1)$
b	176 (20)	*b*	226.5 (54)	*b*	173.6 (14)	$\nu_6(b_2)$

[a] C_{2v} symmetry. [b] Too weak to be detected, obscured by more intense absorptions, or outside the range of detection.

ν(Al−H) stretching vibrations associated with **3a**−**c**. The absorptions are, however, close to two of the absorptions due to HAlClBr, HAlFCl, and HAlFBr, which may indicate some structural similarities. The bands at 881.7 (**3b**) and 871.1 (**3c**) cm^{-1} occur in a region where ν(Al−F) stretching fundamentals of Al(III) species are expected to show. The absorptions at 588 (**3a**) and 627.1 (**3b**) cm^{-1} are strong candidates for ν(Al−Cl) stretching fundamentals. Finally, the absorptions at 511 (**3a**) and 522.2 (**3c**) cm^{-1} occur in a region characteristic of ν(Al−Br) stretching modes. The obvious inference is that **3a**−**c** are the mixed Al(III) halides $AlClBr_2$, $AlFCl_2$, and $AlFBr_2$. Of these, only $AlClBr_2$ has to our knowledge been studied previously in matrix isolation experiments,[30] and the reported vibrational properties tally nicely with those observed here.

DFT calculations were employed to characterize further these species. Like HAlClBr, HAlFCl, or HAlFBr, the molecules exhibit a planar global energy minimum structure, this time resulting in C_{2v} symmetry. Because of the increased electronegativities of its ligands, the Al−F distances of $AlFCl_2$ and $AlFBr_2$ are slightly shorter than those of HAlFCl and HAlFBr, respectively. For the same reason, the Al−Cl distance in $AlFCl_2$ is shorter than those in HAlFCl, HAlClBr, or $AlClBr_2$ (see below and Table 10 for a more detailed evaluation of the structures).

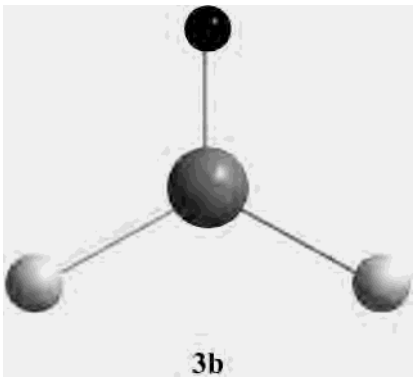

3b

Table 5 compares the experimental IR properties with those calculated for the molecules in their global energy minimum structure. Two of the six vibrational modes of the molecules were detected. For $AlClBr_2$ (**3a**), absorptions were observed at 588 and 511 cm^{-1}. The mode at 588 cm^{-1} can be assigned to the antisymmetric Al−Br stretching mode, $\nu_4(b_1)$, which is calculated to appear at 581 cm^{-1}. The absorption at 511 cm^{-1} belongs to the Al−Cl stretching fundamental, $\nu_1(a_1)$; the calculations predict a wavenumber of 507 cm^{-1} for this mode. The absorptions due to $AlFCl_2$ (**3b**) at 881.7 and 627.1 cm^{-1} can then be assigned to the symmetric Al−F stretching fundamental, $\nu_1(a_1)$, and the antisymmetric Al−Cl stretching mode, $\nu_4(b_1)$, for which the calculations yielded wavenumbers of 880.5 and 629.8 cm^{-1}, respectively. These two modes carry most of the IR intensity. Finally, bands at 871.1 and 522.2 cm^{-1} were assigned to product **3c**. Of these, the band at 871.1 cm^{-1} can again be assigned to the ν(Al−F) stretching mode $\nu_1(a_1)$, which is, as anticipated, only slightly affected by replacement of the two Cl atoms by Br atoms. The experimental value is in good agreement with the calculated one (865.0 cm^{-1}). The band that carries most of the intensity can be attributed to the antisymmetric Al−Br stretching mode, $\nu_4(b_1)$. Our calculations resulted in a wavenumber of 517.2 cm^{-1} for this mode.

Table 6. Comparison between the IR Absorptions Observed and Calculated for $AlCl_2Br$ (**4a**), AlF_2Cl (**4b**), and AlF_2Br (**4c**) [wavenumbers in cm^{-1}, with calculated IR intensities (in km mol^{-1}) in parentheses]

$AlCl_2Br$ (**4a**)		AlF_2Cl (**4b**)		AlF_2Br (**4c**)		
exptl	calcd[a]	exptl	calcd[a]	exptl	calcd[a]	assignment
560.1	556 (148)	831.3	826.4 (144)	831.1	808.2 (143)	$\nu_1(a_1)$
b	314 (6)	*b*	496.4 (34)	*b*	396.9 (52)	$\nu_2(a_1)$
b	131 (5)	*b*	221.9 (29)	*b*	202.5 (21)	$\nu_3(a_1)$
616.1	610 (137)	887.1	945.6 (110)	873.6	940.3 (102)	$\nu_4(b_1)$
b	187 (26)	*c*	193.7 (13)	*c*	172.2 (8)	$\nu_5(b_1)$
b	119 (4)	*b*	259.6 (83)	*b*	260.3 (71)	$\nu_6(b_2)$

[a] C_{2v} symmetry. [b] Too weak to be detected, obscured by more intense absorptions, or outside the range of detection.

$AlCl_2Br$, AlF_2Cl, and AlF_2Br, 4a−c. The IR spectra gave evidence for a fourth reaction product. The absorptions at 616.1 and 560.1 cm^{-1} due to species **4a** occur in a region characteristic of ν(Al−Cl) stretching modes. The absorptions at 887.1 and 831.3 cm^{-1} (**4b**) and at 873.6 and 831.1 cm^{-1} (**4c**) most likely belong to ν(Al−F) stretching fundamentals. The detection of two Al−Cl modes of **4a** and two Al−F modes of **4a** and **4b** (asymmetric and symmetric stretching fundamentals) indicates the presence of two Cl atoms in **4a** and two F atoms in **4b** and **4c**. Therefore **4a**−**c** are likely to be the Al(III) halides $AlCl_2Br$, AlF_2Cl, and AlF_2Br.

Calculations were again performed to simulate the IR properties. Table 6 includes a comparison between the wavenumbers observed and calculated for these species. In pleasing agreement with the experimental results, the calculations predict the symmetric and antisymmetric Al−Cl ($AlCl_2Br$) and Al−F (AlF_2Cl and AlF_2Br) stretching modes to give rise to the most intense absorptions in the IR spectrum. With wavenumbers of 610 and 556 ($AlCl_2Br$), 945.6 and 826.4 (AlF_2Cl), and 940.3 and 808.2 cm^{-1}, the calculated wavenumbers are in fair agreement with the observed ones.

Comparison between the Structures of the Characterized Al(III) Species. Table 7 compares the dimensions for

(30) Pong, R. G. S.; Shirk, A. E.; Shirk, J. S. *J. Chem. Phys.* **1979**, *70*, 525.

Table 7. Calculated Distances (in Å) and Bond Angles (in deg) of the Al(III) Species Studied in This Work

	HAlClBr	HAlFCl	HAlFBr	$AlClBr_2$	$AlFCl_2$	$AlFBr_2$	$AlCl_2Br$	AlF_2Cl	AlF_2Br
Al−H	1.5844	1.5748	1.5762						
Al−F		1.6724	1.6741		1.6651	1.6680		1.6608	1.6621
Al−Cl	2.1091	2.1022		2.1000	2.0890		2.0974	2.0827	2.2333
Al−Br	2.2610		2.2551	2.2495		2.2437	2.2464		
H−Al−F		119.9	119.3						
H−Al−Cl	120.1	122.6							
H−Al−Br	121.1		122.7						
F−Al−F								118.1	118.6
F−Al−Cl		117.5			119.1			120.7	
F−Al−Br			118.0			118.8			120.9
Cl−Al−Cl					121.8		119.2		
Cl−Al−Br	118.9			119.7			120.4		
Br−Al−Br				120.6		122.5			

all Al(III) species studied in this work. From this comparison it can be seen how the different electronegativities of the ligands influence the bond distances and the bond angles. The bond lengths are short if the overall electronegativity of the ligands is high. Thus, e.g., the Al−F bond length is shortest in AlF_2Cl, which exhibits the highest overall electronegativity of its ligands and increases in the order $AlF_2Cl < AlF_2Br < AlFCl_2 < AlFBr_2 <$ HAlFCl < HAlFBr. The force constants *f*(Al−F) follow the opposite trend, decreasing in the row $AlF_2Cl > AlF_2Br > AlFCl_2 > AlFBr_2$ > HAlFCl > HAlFBr. In HAlFCl, for example, *f*(Al−F) amounts to 501 N m^{-1}, but in HAlFBr it is reduced to 423 N m^{-1}. The Al−H, Al−Cl, and Al−Br bond lengths follow the same pattern. Additionally, the bond angles are small if ligands with high electronegativities are involved, in agreement with the predictions made by the VSEPR model.[23] Thus in HAlFCl, for example, the bond angles follow the order F−Al−Cl < H−Al−F < H−Al−Cl, reflecting the increasing electronegativity in the direction H < Cl < F. The largest bond angle is adopted for H−Al−Br in HAlFBr (122.7°), which features the combination of atoms with the smallest total electronegativity.

Reaction Pathways. AlCl and AlF have each been shown to form an adduct of the form AlX·HY (X = F or Cl, Y = Cl or Br) upon co-deposition together with HCl or HBr in a solid Ar matrix. These adducts are photolabile and undergo conversion to the Al(III) hydrides HAlXY upon UV photolysis (λ = ca. 254 nm). The overall photoinduced reactions of AlF with HCl or HBr to give the Al(III) species HAlFCl and HAlFBr, respectively, and of AlCl with HBr to give HAlClBr (see eq 3) proceed exothermally, the calculated reaction energies being −204.7, −197.4, and −214 kJ mol^{-1}, respectively.

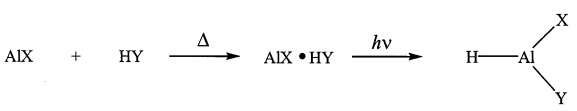

(3)

In addition to HAlClBr, HAlFCl, and HAlFBr, the experiments gave evidence for the photoinduced formation of $AlClBr_2$, $AlFCl_2$, and $AlFBr_2$ (**3a**−**c**). These species are most likely the products of the reaction of AlCl and AlF with two molecules of HBr or HCl. A possible route to these species starts with the bisadducts $AlCl(HBr)_2$, $AlF(HCl)_2$, and $AlCl(HBr)_2$, which eliminate dihydrogen upon photoactivation (see eq 4). Experiments with Al atoms and NH_3

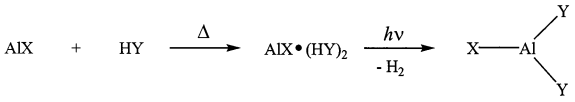

(4)

molecules gave evidence for the Al(II) bisamide $Al(NH_2)_2$, which is, in the same way, likely to be formed by photoinduced hydrogen elimination from the bisadduct $Al(NH_3)_2$.[31] The reactions yielding $AlClBr_2$, $AlFCl_2$, and $AlFBr_2$ and dihydrogen were calculated to be exothermic by −347, −330.8, and −317.6 kJ mol^{-1}.

Under the conditions of the experiments, there also appeared weak IR absorptions which can be assigned to the mixed halides $AlCl_2Br$, AlF_2Cl, and AlF_2Br (**4a**−**c**). $AlCl_2$-Br is most likely formed as a product of the reaction of AlCl with both HBr and HCl, the latter being present in traces due to incomplete reaction with liquid Al in the Knudsen cell. In the same way, AlF_2Cl and AlF_2Br are products of the reactions of AlF and HF with HCl and HBr, respectively. No absorption attributable to a photoproduct of $(AlF)_2$ appears in the IR spectra. Most likely, photolysis achieves decomposition of $(AlF)_2$ to give two AlF molecules, which subsequently react with HCl or HBr in the ways described herein.

Conclusions

In this work the reactions of AlCl with HBr and of AlF with HCl and HBr were studied experimentally in a solid Ar matrix by IR spectroscopy, including the effects of isotopic substitution, and theoretically by quantum chemical calculations. Twelve species were characterized, most of them for the first time. These were the adducts AlCl·HBr, AlF·HCl, and AlF·HBr and the monomeric Al(III) species HAlClBr, HAlFCl, HAlFBr, $AlClBr_2$, $AlFCl_2$, $AlFBr_2$, $AlCl_2$-Br, AlF_2Cl, and AlF_2Br. The adducts AlCl·HBr, AlF·HCl, and AlF·HBr were spontaneously formed upon co-deposition of the reactants. They can be converted by UV photolysis into the new Al(III) hydrides HAlClBr, HAlFCl, and HAlFBr, respectively. In addition, the experiments gave evidence for the presence of $AlClBr_2$ as the product of the

(31) Gaertner, B.; Himmel, H.-J. *Inorg. Chem.* **2002**, *41*, 2496. Kasai, P.; Himmel, H.-J. *J. Phys. Chem. A* **2002**, *106*, 6765.

photoinduced reaction of AlCl with two molecules of HBr, and of $AlFCl_2$ and $AlFBr_2$ as products of the reaction of AlF with two molecules of HCl and HBr, respectively. The trends in the calculated bond lengths and angles were established for all the species addressed in this work. In addition to the characterization of several new monomeric aluminum compounds, this work should shed light on fundamental processes such as the oxidation of aluminum metal by hydrogen halides, e.g. HCl, leading in several steps to $AlCl_3$.

Acknowledgment. The authors thank the Deutsche Forschungsgemeinschaft for financial support and the award of a Habilitationsstipendium to H.-J. H.

IC020275A